arXiv:1504.00059v2 [cond-mat.mes-hall] 20 Sep 2016

Quantum Adiabatic Pumping by Modulating Tunnel Phase in Quantum Dots

Masahiko Taguchi[1], Satoshi Nakajima[1], Toshihiro Kubo[1], and Yasuhiro Tokura[1,2]*

[1]*Graduate School of Pure and Applied Sciences, University of Tsukuba, 1-1-1 Tennodai, Tsukuba, Ibaraki 305-8571, Japan*

[2]*NTT Basic Research Laboratories, NTT Corporation, 3-1 Morinosato-Wakamiya, Atsugi, Kanagawa 243-0198, Japan*

In a mesoscopic system, under zero bias voltage, a finite charge is transferred by quantum adiabatic pumping by adiabatically and periodically changing two or more control parameters. We obtained expressions for the pumped charge for a ring of three quantum dots (QDs) by choosing the magnetic flux penetrating the ring as one of the control parameters. We found that the pumped charge shows a steplike behavior with respect to the variance of the flux. The value of the step heights is not universal but depends on the trajectory of the control parameters. We discuss the physical origin of this behavior on the basis of the Fano resonant condition of the ring.

1. Introduction

Recently, quantum adiabatic pumping has attracted much attention.[1–6] Quantum adiabatic pumping induces a finite current in a mesoscopic system at zero bias voltage by adiabatically and periodically changing two or more control parameters. Classical pumping based on the Coulomb charging effect such as that in single-electron transistors[7,8] or turnstile devices[9] does not require phase coherence. In contrast, quantum pumping is fundamentally different from classical pumping. Periodic deformation of two or more parts of the potential induces phase-coherent redistribution of the electron charges in an open quantum system. During this redistribution, electrons can be coherently pumped from one lead to the other leads. In spatially periodic systems, Thouless showed quantized charge transport induced by adiabatic and periodic changes in the potential.[10] Later, a formulation using a scattering matrix appeared,[11,12] which is called Brouwer's formula. This formula is most conveniently applied to

*E-mail: tokura.yasuhiro.ft@u.tsukuba.ac.jp

a quantum adiabatic pumping in noninteracting systems. Relative modulating phase of the control parameters (this phase is not a scattering phase, which will appear in the following) in Brouwer's formula determines the magnitude and the sign of the pumped charge. An experimental demonstration of Brouwer's formula has been reported.[13] In this experiment, two gate voltages controlled the periodical deformations of the shape of the quantum dot (QD), and then the pumped current was observed, where the amplitude of the current changed with the relative phase of the two gate voltages, as the theory predicted. However, the result is still open to argument since the pumped current can also be explained by the rectification effect of the displacement currents generated by the time-dependent gate voltages.[14–18]

In addition to the experimental studies, there have been several detailed theoretical studies on Brouwer's formula. For example, the maximum value of the pumped charge per cycle becomes exactly an elementary charge[19] by appropriately choosing two potentials as control parameters in one QD system. The effect of the resonance on the quantum adiabatic pumping has been analyzed in a double-barrier quantum well[20] and a QD in a turnstile geometry.[21] The effect of dephasing has also been studied.[22,23] In two-terminal systems, the scattering matrix is given by a 2×2 unitary matrix, and there are four independent real parameters in this matrix. Avron *et al*. clarified the roles of each parameter in the transport process.[24] Additionally, the inverse process, namely, adiabatic quantum motors driven by applying finite bias, has been analyzed with scattering matrix formalisms.[25]

As discussed above, there have been many studies on quantum adiabatic pumping with modulating potentials. However, there have been no studies on choosing *a scattering phase* as one of the control parameters. Avron *et al*. considered the role of the phase in quantum transport in a general framework.[24] However, there seem to be no studies based on an explicit model system. On the other hand, the quantum mechanical phase plays an important role in the field of quantum transport. The Josephson effect[26] is one of the examples, where the current occurs owing to the difference in the phase of macroscopic wave functions. The electron phase is a quantum mechanical value, and electrons obtain the phase by transport in the scattering region, e.g., QDs. Choosing the phase as one of the control parameters is physically interesting because the phase can be related to the local bias voltage between QDs (e.g., Faraday's law of electromagnetic induction).[27] The effect of the time-dependent vector potential on the electrons in a metallic system has been explored.[28–30] Also, quantum adiabatic pumping using the ac Josephson effect has been proposed.[31] To investigate how the periodicity and quantum property of the phase appear in the transport process, we analyze quantum adiabatic pumping by choosing a tunnel phase as one of the control parameters.

We treat a three-QD ring, where the modulation of the tunnel phase is equivalent to the modulation of the Aharonov–Bohm (AB) flux penetrating through the ring. The effect of the nonadiabatic modulation of the AB flux on the transport of the ring has been studied.[32–34] Moreover, quantum adiabatic pumping with a single control parameter under a finite AB flux has been examined.[35] If we choose one QD energy level and the flux penetrating through the ring as control parameters, the pumped charge becomes a sinusoidal form or a steplike form as a function of the variance of the phase, depending on the values of the system parameters (the energy levels of QDs, the tunnel strengths). For the parameters realizing steplike behavior, there is no upper bound of the pumped charge.

The structure of this paper is as follows. In Sect. 2, we explain theoretical model and formal solutions. In Sect. 3, we numerically analyze quantum adiabatic pumping in a three-QD ring, choosing the energy level of one QD and the flux penetrating through the ring as control parameters. In Sect. 4, we analytically discuss the origin of the singular behavior of the kernel under the condition of weak couplings to the leads. Finally, in Sect. 5, we conclude the paper. In the Appendix, we provide the derivation of the kernel of the three-QD ring.

2. Model

2.1 Hamiltonian

In this section, we explain the model considered in this study, where a QD system is coupled to two leads, as shown in Fig. 1. The left and right leads couple to QD1 and QD2, respectively. We considered only a single level in each QD. We disregarded the spin degree of freedom of electrons and ignored inter-QD Coulomb interactions. Because we treated only a single level in each QD and did not consider the spin degree of freedom, then, according to the Pauli exclusion principle, the occupied electron number is 0 or 1; therefore, we did not need to consider intra-QD interactions.

The Hamiltonian $\hat{H} = \hat{H}_{\rm QDs} + \hat{H}_{\rm leads} + \hat{H}_{\rm T}$ consists of the QD system part $\hat{H}_{\rm QDs}$, the non-interacting lead part $\hat{H}_{\rm leads}$, and $\hat{H}_{\rm T}$ representing tunnel couplings between leads and QDs:

$$\hat{H}_{\rm QDs} = \sum_{i=1}^{3} \varepsilon_i \hat{d}_i^\dagger \hat{d}_i + \sum_{i,j=1,i\neq j}^{3} t_{ij} \hat{d}_i^\dagger \hat{d}_j, \tag{1}$$

$$\hat{H}_{\rm leads} = \sum_{\alpha=L,R} \sum_{k} \varepsilon_{\alpha k} \hat{C}_{\alpha k}^\dagger \hat{C}_{\alpha k}, \tag{2}$$

$$\hat{H}_{\rm T} = \sum_{k} \left\{ V_{Lk} \hat{C}_{Lk}^\dagger \hat{d}_1 + V_{Rk} \hat{C}_{Rk}^\dagger \hat{d}_2 \right\} + \text{h.c.} \tag{3}$$

Here, i and j are the indices of the QDs. $\hat{d}_i^\dagger \left(\hat{d}_i\right)$ is a creation (annihilation) operator of a

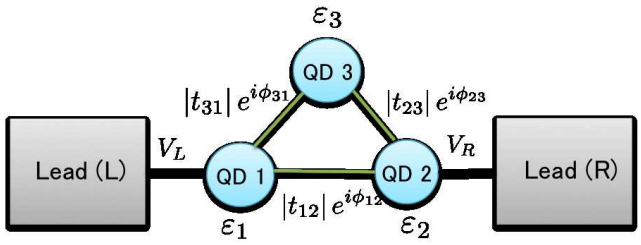

Fig. 1. (Color online) Schematic of the three-QD ring.

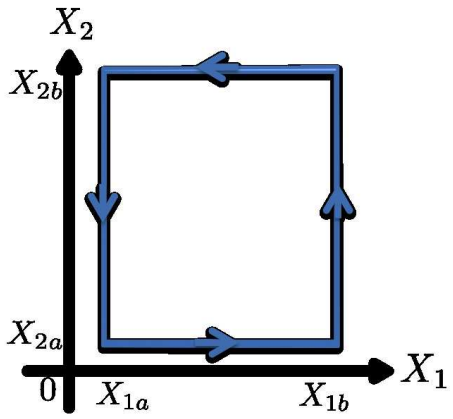

Fig. 2. (Color online) Trajectory of two control parameters.

localized electron in the ith QD. ε_i is the energy level of the ith QD. The tunnel couplings between the ith and jth QDs, $t_{ij}\left(=t_{ji}^{*}\right)$, have a Peierls phase ϕ_{ij} as $t_{ij} \equiv \left|t_{ij}\right| e^{i\phi_{ij}}$. $\hat{C}_{\alpha k}^{\dagger}\left(\hat{C}_{\alpha k}\right)$ is a creation (annihilation) operator of an electron of energy $\varepsilon_{\alpha k}$ with wave number k in lead α. $V_{\alpha k}$ is the tunnel coupling amplitude. We examine the model at zero bias voltage and under a zero-temperature condition.

2.2 Method

Let X_1 and X_2 be two independent control parameters. We change the two parameters X_1 and X_2 on the rectangular trajectory shown in Fig. 2 along the arrow. The expression for the pumped charge per cycle was introduced by Büttiker *et al*.[11] and formulated by Brouwer,[12] which is given by an oriented surface integral of the kernel Π over the area depicted in Fig. 2 in the X_1-X_2 phase space,

$$\frac{Q}{-e} \equiv q = -\int_{X_{1a}}^{X_{1b}} \int_{X_{2a}}^{X_{2b}} dX_1 dX_2\, \Pi\left(X_1, X_2\right), \tag{4}$$

where q indicates the number of pumped electrons from lead R to lead L per cycle and e is an elementary charge. In the following, we call q the pumped charge. $\Pi(X_1, X_2)$ is the kernel expressed by the scattering matrix $\mathbf{S}$, which is a function of two control parameters,

$$\Pi(X_1, X_2) = \frac{1}{\pi}\mathrm{Im}\left\{\frac{\partial S_{LL}^*}{\partial X_1}\frac{\partial S_{LL}}{\partial X_2} + \frac{\partial S_{LR}^*}{\partial X_1}\frac{\partial S_{LR}}{\partial X_2}\right\}. \tag{5}$$

The components of the scattering matrix are given by retarded Green's functions through the Fisher–Lee relation,[36–38]

$$S_{LL} = 1 - i\Gamma_L G_{11}^r(\varepsilon_F), \tag{6}$$

$$S_{LR} = -i\sqrt{\Gamma_L\Gamma_R}G_{12}^r(\varepsilon_F). \tag{7}$$

Γ_α ($\alpha = L$ or R) is the line width defined by $\Gamma_\alpha \equiv 2\pi\rho_\alpha |V_\alpha|^2$ with the wide-band limit (ignoring the energy dependence of the line width), where ρ_α is the density of states of lead α. The retarded Green's function of the QD system, $G_{nm}^r(\varepsilon)$, is defined by the Fourier transformation of

$$G_{nm}^r(t, t') \equiv -\frac{i}{\hbar}\theta(t - t')\left\langle\left\{\hat{d}_n(t), \hat{d}_m^\dagger(t')\right\}\right\rangle, \tag{8}$$

where $n, m = 1, 2, 3$ and $\theta(t)$ is the step function. The operators are in the Heisenberg picture [e.g., $\hat{d}_n(t) \equiv e^{i\hat{H}t/\hbar}\hat{d}_n e^{-i\hat{H}t/\hbar}$] and $\langle\cdots\rangle$ denotes the quantum mechanical and statistical average at zero temperature. Since we consider zero bias voltage and zero temperature condition, the energy of the incident electrons, ε, is set to the Fermi energy ε_F. Hence, the kernel can be obtained with the retarded Green's function:

$$\Pi(X_1, X_2) = \frac{1}{\pi}\mathrm{Im}\left\{\Gamma_L^2\frac{\partial G_{11}^{r*}(\varepsilon_F)}{\partial X_1}\frac{\partial G_{11}^r(\varepsilon_F)}{\partial X_2} + \Gamma_L\Gamma_R\frac{\partial G_{12}^{r*}(\varepsilon_F)}{\partial X_1}\frac{\partial G_{12}^r(\varepsilon_F)}{\partial X_2}\right\}. \tag{9}$$

Using the equation of motion method, the Fourier transform of the retarded Green's function of the three-QD ring is given by

$$\mathbf{G}^r(\varepsilon) = \begin{pmatrix} \varepsilon - \varepsilon_1 + \frac{i}{2}\Gamma_L & -t_{12} & -t_{13} \\ -t_{21} & \varepsilon - \varepsilon_2 + \frac{i}{2}\Gamma_R & -t_{23} \\ -t_{31} & -t_{32} & \varepsilon - \varepsilon_3 \end{pmatrix}^{-1}. \tag{10}$$

We derive the kernel Eq. (9) choosing the energy of QD 3, ε_3, and the AB phase ϕ_{AB} from the magnetic flux penetrating through the ring as control parameters. Details of the calculation are given in the Appendix. To make the notation simpler, we introduce the dimensionless parameters $x_1 \equiv \frac{\varepsilon_F - \varepsilon_1}{\Gamma_L}$, $x_2 \equiv \frac{\varepsilon_F - \varepsilon_2}{\Gamma_R}$, $x_3 \equiv \frac{\varepsilon_F - \varepsilon_3}{\gamma}$, $s_{12} \equiv \frac{t_{12}}{\sqrt{\Gamma_L\Gamma_R}}$, $s_{23} \equiv \frac{t_{23}}{\sqrt{\Gamma_R\gamma}}$, and $s_{31} \equiv \frac{t_{31}}{\sqrt{\Gamma_L\gamma}}$, where we have introduced a positive constant γ to normalize the energy of QD 3 ε_3 (the choice of γ does not affect the result). We also introduce the normalized kernel $\tilde{\Pi}(x_3, \phi_{\mathrm{AB}}) \equiv \gamma\Pi(\varepsilon_3, \phi_{\mathrm{AB}})$,

and the pumped charge is obtained by

$$q = -\int_{x_{3\min}}^{x_{3\max}} dx_3 \int_{\phi_{\mathrm{ABmin}}}^{\phi_{\mathrm{ABmax}}} d\phi_{\mathrm{AB}}\, \tilde{\Pi}(x_3, \phi_{\mathrm{AB}}). \tag{11}$$

We can see that the kernel Eq. (A·6) is a periodical function of ϕ_{AB}. Regarding the normalized kernel $\tilde{\Pi}(x_3, \phi_{\mathrm{AB}})$ as a function of $(x_1, x_2, |s_{23}|, |s_{31}|, \phi_{\mathrm{AB}})$, we found the following symmetry:

$$\tilde{\Pi}(x_3, \phi_{\mathrm{AB}})\big|_{x_1, x_2, |s_{23}|, |s_{31}|} = \tilde{\Pi}(x_3, -\phi_{\mathrm{AB}})\big|_{x_2, x_1, |s_{31}|, |s_{23}|}, \tag{12}$$

which is related to the symmetry of time and space reversal. Moreover, regarding the kernel $\tilde{\Pi}(x_3, \phi_{\mathrm{AB}})$ as a function of $(x_1, x_2, x_3, \phi_{\mathrm{AB}})$, there is another symmetry,

$$\tilde{\Pi}(x_3, \phi_{\mathrm{AB}})\big|_{x_1, x_2} = -\tilde{\Pi}(-x_3, \pi - \phi_{\mathrm{AB}})\big|_{-x_1, -x_2}, \tag{13}$$

which is related to the electron-hole symmetry.

3. Numerical Results

In this section, we present the numerical results of the kernel and pumped charge Q. In Figs. 3 and 4, we show the contour plots of the kernel $\tilde{\Pi}(x_3, \phi_{\mathrm{AB}})$ and the corresponding pumped charge q as a function of the upper bound of the phase ϕ_{ABmax}. The integration region of the AB phase is $-\pi \le \phi_{\mathrm{AB}} \le \phi_{\mathrm{ABmax}}$. We set the normalized tunnel couplings to $|s_{12}| = |s_{23}| = |s_{31}| = 1$. Figure 3 corresponds to normalized energies of QDs 1 and 2 being the same ($x_1 = x_2 = 0.1$), and Fig. 4 corresponds to normalized energies of QDs 1 and 2 being opposite ($x_1 = -x_2 = 0.1$). In Figs. 3(c) and 4(c), the solid lines represent the integration region $-3 \le x_3 \le 3$ of the kernel and the dashed lines represent the integration region $-6 \le x_3 \le 6$. Positive and negative peaks appear (almost) periodically in the direction of the phase in the contour plot of the kernel. When the signs of the energies of QDs 1 and 2 are the same, the peak heights are smaller than the depth of the negative peaks (Fig. 3), and the pumped charges become increasingly negative with ϕ_{ABmax} on average. When the signs of the energies of QDs 1 and 2 are opposite, the peak heights and depths are the same (Fig. 4). Then the pumped charge per cycle is periodical as a function of ϕ_{ABmax} and a sinusoidal form. We can understand this behavior for $x_1 = -x_2 = 0.1$ by considering the two symmetries, Eqs. (12) and (13), $\tilde{\Pi}(x_3, \phi_{\mathrm{AB}})\big|_{x_1, x_2} = \tilde{\Pi}(x_3, -\phi_{\mathrm{AB}})\big|_{x_2, x_1} = -\tilde{\Pi}(-x_3, \phi_{\mathrm{AB}} + \pi)\big|_{-x_2, -x_1}$ (note that $|s_{12}| = |s_{23}| = |s_{31}| = 1$). In Figs. 3(d) and 4(d), the solid lines are the results for the integration region $0 \le x_3 \le 3$ of the kernel, and the dashed lines are for the integration region $0 \le x_3 \le 6$. When we choose the integration region to pick up only negative peaks, the corresponding pumped charge shows a steplike form as a function of ϕ_{ABmax}. There is no upper (or lower) bound of the pumped charge per cycle, except for the special situation explained above.

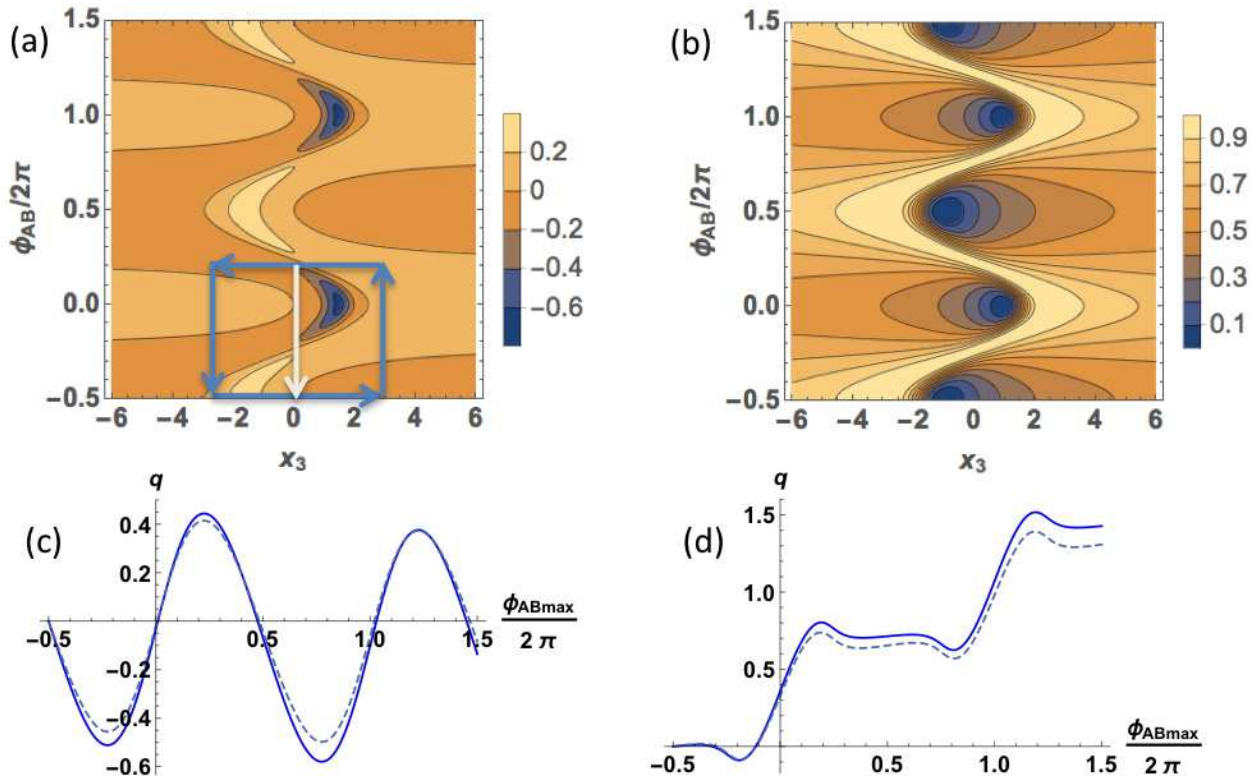

Fig. 3. (Color online) (a) Contour plots of normalized kernel $\tilde{\Pi}(x_3, \phi_{AB})$ and (b) transmission probability of the three-QD ring (the horizontal axis is the normalized energy of QD 3 x_3 and the vertical axis is the phase ϕ_{AB} in unit of 2π.) The color bar indicates the value of the kernel and the probability. We set normalized tunnel couplings $|s_{12}| = |s_{23}| = |s_{31}| = 1$. The normalized energies of QDs 1 and 2 are the same ($x_1 = x_2 = 0.1$). Arrows in (a) indicate the trajectory of the parameters. (c) and (d) Pumped charges (the horizontal axis is the upper bound of the phase ϕ_{ABmax} and the vertical axis is the pumped charge q): in (c) solid lines represent the integration region $-3 \le x_3 \le 3$ of the kernel, and dashed lines represent the integration region $-6 \le x_3 \le 6$; in (d) solid lines represent the integration region $0 \le x_3 \le 3$ of the kernel, and dashed lines represent the integration region $0 \le x_3 \le 6$.

We found very different behavior of the kernel at a special choice of the parameters. In the following, we restrict ourselves to the symmetric situation $|s_{12}| = |s_{23}| = |s_{31}| = Z$. When $x_1 = x_2 = Z$, there are a series of isolated dips at $x_3 = Z$ and $\phi_{AB} = 2n\pi$ with an integer n. Figures 5(a) and 5(b) show the contour plot of the kernel $\tilde{\Pi}(x_3, \phi_{AB})$ and the transmission probability under the condition $Z = 1$, respectively. Figure 5(c) shows the pumped charge. The solid line represents the integration region $0.7 \le x_3 \le 1.3$, and the dashed line represents the integration region $0 \le x_3 \le 2$. Because of isolated structures in the kernel, the pumped charge per cycle becomes steplike as a function of the upper bound of the phase ϕ_{ABmax}. This behavior means that the pumped charge is quantized and is robust against the uncertainty of the phase. Using the symmetry Eq. (13), we have a series of isolated *peaks* at $\phi_{AB} = (2n + 1)\pi$

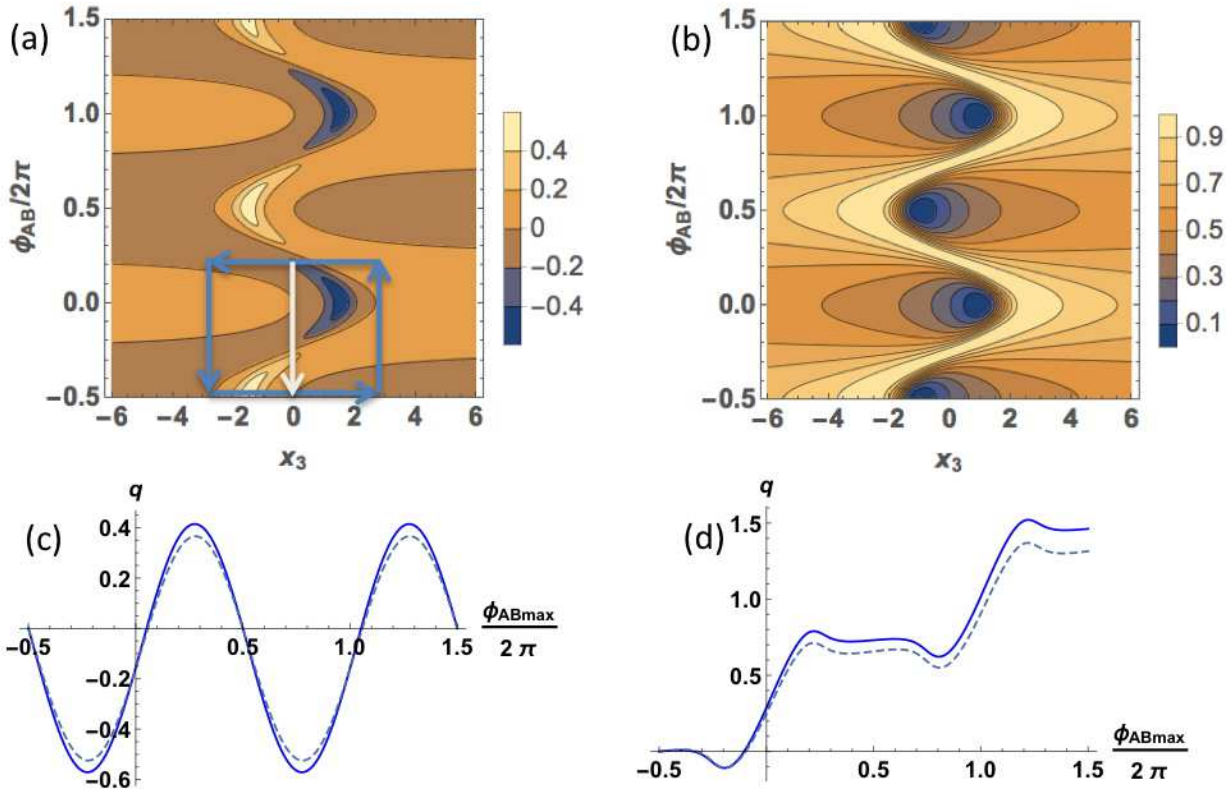

Fig. 4. (Color online) Similar plot to Fig. 3 except for the normalized energies of QDs 1 and 2 being the opposite sign ($x_1 = -x_2 = 0.1$).

(n: integer) and $x_3 = -Z$ when $x_1 = x_2 = -Z$.

4. Discussion

The origin of these peaks/dips of the kernel can be understood as the resonance behavior of the scattering matrix. The transmission probability of this three-QD ring is

$$\mathcal{T} = \frac{1}{|\Delta_3|^2}\left|x_3\,|s_{12}| - |s_{23}s_{31}|\,e^{-i\phi_{AB}}\right|^2, \tag{14}$$

where the factor Δ_3 is defined in the Appendix by Eq. (A·7). The kernel also depends on this factor $\tilde{\Pi} \propto |\Delta_3|^{-4}$. Therefore, both the transmission probability and the kernel are enhanced when $|\Delta_3|$ is strongly suppressed (quasi-resonant condition). We rewrite this factor as

$$\begin{aligned}\Delta_3 \;=\; & \left(x_1x_2 - |s_{12}|^2 - \frac{1}{4}\right)x_3 + 2|s_{12}s_{23}s_{31}|\cos\phi_{AB} - \left(|s_{23}|^2x_1 + |s_{31}|^2x_2\right) \\ & + \frac{i}{2}\left[(x_1+x_2)x_3 - |s_{23}|^2 - |s_{31}|^2\right].\end{aligned} \tag{15}$$

On the basis of the numerical results shown in the previous section, we consider the condition of weakly coupled triple QDs to the leads, namely, $|s_{12}|, |s_{23}|, |s_{31}| \gg 1$. Let us discuss the

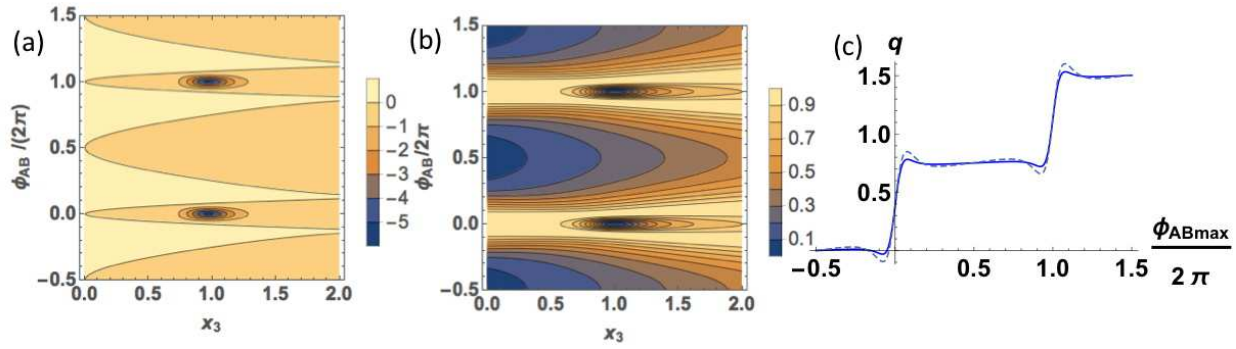

Fig. 5. (Color online) (a) Contour plot of the kernel $\tilde{\Pi}(x_3, \phi_{AB})$ and (b) transmission probability $\mathcal{T}$ (the horizontal axis is the normalized energy of QD 3 x_3 and the vertical axis is the phase ϕ_{AB}). (c) Pumped charge (the horizontal axis is the upper bound of the phase ϕ_{ABmax} and the vertical axis is the pumped charge q). The solid line represents the integration region of $0.7 \leq x_3 \leq 1.3$, and the dashed line represents that for $0 \leq x_3 \leq 2$. We set the normalized tunnel coupling and the energies of QDs 1 and 2 to $|s_{12}| = |s_{23}| = |s_{31}| = x_1 = x_2 = 1$.

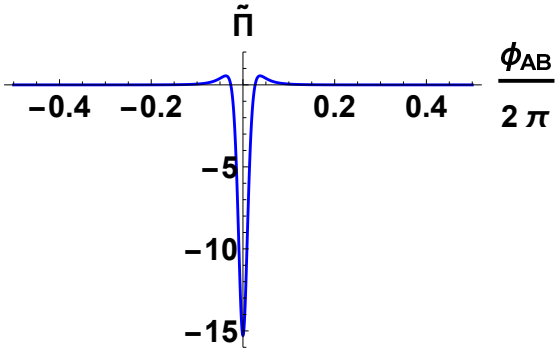

Fig. 6. (Color online) Kernel $\tilde{\Pi}$ as a function of ϕ_{AB} at $|s_{12}| = 3$ and $\beta = 1$.

origin of the sharp isolated dip found for all positive x_1, x_2, and x_3. In order to obtain isolated dips, Δ_3 should be strongly suppressed at $\phi_{AB} = 2n\pi$ (When x_1, x_2, and x_3 are all negative, resonance occurs when $\phi_{AB} = (2n+1)\pi$). Then we require that the third term in Eq. (15), which is independent of x_3, becomes $2|s_{12}s_{23}s_{31}|$ and we have

$$x_2 = \frac{1}{|s_{31}|^2}\left(2|s_{12}s_{23}s_{31}| - |s_{23}|^2 x_1\right),$$

By substituting this relation into the first term, the coefficient of x_3 becomes

$$x_1x_2 - |s_{12}|^2 - \frac{1}{4} = -\left(\left|\frac{s_{23}}{s_{31}}\right| x_1 - |s_{12}|\right)^2 - \frac{1}{4}. \tag{16}$$

Therefore, the real part of Δ_3 becomes very small at $x_1 = \left|\frac{s_{12}s_{31}}{s_{23}}\right|$ and $x_2 = \left|\frac{s_{12}s_{23}}{s_{31}}\right|$. The resonant condition is achieved at the value of x_3 where the imaginary part of Eq. (15) becomes zero:

$$(x_1 + x_2)x_3 = |s_{23}|^2 + |s_{31}|^2,$$

$$\rightarrow \quad x_3 = \left| \frac{s_{23}s_{31}}{s_{12}} \right|. \tag{17}$$

Figure 5(b) shows the transmission probability as a function of the two control parameters. Clearly, near the condition of a sharp dip of the kernel, the transmission probability is strongly enhanced, but becomes zero exactly at the condition of the sharp dip of the kernel (in Fig. 5, $x_3 = 1, \phi_{\rm AB} = 0, 2\pi$). This sharp dip of the conductance near the resonant conditions can be understood as *Fano resonance*, where the continuum spectra of the leads and the discrete energy level of the three-QD ring interfere.

Then we introduce the offset variable a to study the behavior of the kernel near the resonant dip, defined as $a \equiv x_3 - \left|\frac{s_{23}s_{31}}{s_{12}}\right|$ and fix $x_1 = \left|\frac{s_{12}s_{31}}{s_{23}}\right|$ and $x_2 = \left|\frac{s_{12}s_{23}}{s_{31}}\right|$. We estimate the transmission probability and the kernel for $|s_{12}|, |s_{23}|, |s_{31}| \gg 1$, with neglecting a small term, namely, the factor -1/4 in the first bracket of Eq. (15) times a. The transmission probability reads

$$\mathcal{T} \quad \sim \quad |s_{12}|^2 \frac{4\left(1 + \left|\frac{s_{12}a}{s_{23}s_{31}}\right|\right)\sin^2\frac{\phi_{\rm AB}}{2} + \left|\frac{s_{12}a}{s_{23}s_{31}}\right|^2}{\left(\frac{|s_{12}|^2}{2}\left(\frac{1}{|s_{23}|^2} + \frac{1}{|s_{31}|^2}\right)a\right)^2 + \left(\frac{1}{4} + F_{\phi_{\rm AB}}^2\right)^2}, \tag{18}$$

where $F_{\phi_{\rm AB}} \equiv 2|s_{12}|\sin\frac{\phi_{\rm AB}}{2}$, and hence Fano resonance is expected near $a \sim 0$ and $\phi_{\rm AB} = 2n\pi$. Similarly, the kernel is

$$\tilde{\Pi}(a, \phi_{\rm AB}) \quad \sim \quad -\frac{|s_{12}|^3}{\pi|s_{23}s_{31}|} \frac{(\frac{1}{4} + F_{\phi_{\rm AB}}^2)\left\{(\frac{1}{4} - F_{\phi_{\rm AB}}^2)\cos\phi_{\rm AB} + K\sin\phi_{\rm AB}\right\} - a^2 L\sin^2\frac{\phi_{\rm AB}}{2}}{\left\{\left(\frac{|s_{12}|^2}{2}\left(\frac{1}{|s_{23}|^2} + \frac{1}{|s_{31}|^2}\right)a\right)^2 + \left(\frac{1}{4} + F_{\phi_{\rm AB}}^2\right)^2\right\}^2}, \tag{19}$$

where $K \equiv \frac{|s_{12}|}{2}\left(\left|\frac{s_{31}}{s_{23}}\right| - \left|\frac{s_{23}}{s_{31}}\right|\right)$, $L \equiv \frac{1}{2}\left|\frac{s_{12}}{s_{23}s_{31}}\right|^2\left(\left|\frac{s_{23}}{s_{31}}\right|^2 + \left|\frac{s_{31}}{s_{23}}\right|^2\right)$, and we have neglected the terms of the first order of a in the numerator since it means no contribution to the pumped charge when integrated in the range $-a_{\rm max} \le a \le a_{\rm max}$. In the following discussions, we restrict ourselves to the symmetric situation, $|s_{23}| = |s_{31}| \equiv \beta|s_{12}|$, then the kernel becomes simpler,

$$\tilde{\Pi}(a, \phi_{\rm AB}) \quad \sim \quad -\frac{|s_{12}|}{\pi\beta^2} \frac{\left(\frac{1}{4} + F_{\phi_{\rm AB}}^2\right)\left(\frac{1}{4} - F_{\phi_{\rm AB}}^2\right)\cos\phi_{\rm AB} - \left(\frac{a}{\beta^2}\right)^2\sin^2\frac{\phi_{\rm AB}}{2}}{\left\{\left(\frac{a}{\beta^2}\right)^2 + \left(\frac{1}{4} + F_{\phi_{\rm AB}}^2\right)^2\right\}^2}. \tag{20}$$

At $\phi_{\rm AB} = 2n\pi$,

$$\tilde{\Pi}(a, 2n\pi) \quad \sim \quad -\frac{|s_{12}|}{\pi\beta^2} \frac{16}{\left\{\left(\frac{4a}{\beta^2}\right)^2 + 1\right\}^2}, \tag{21}$$

and the kernel has simple dips at $a = 0$, whose width is relatively broad as $\frac{\beta^2}{2}\sqrt{\sqrt{2} - 1} \sim$

$0.32\beta^2$. At $a = 0$,

$$\tilde{\Pi}(0, \phi_{\rm AB}) \quad \sim \quad -\frac{|s_{12}|}{\pi\beta^2}\frac{\left(\frac{1}{4} - F_{\phi_{\rm AB}}^2\right)\cos\phi_{\rm AB}}{\left(\frac{1}{4} + F_{\phi_{\rm AB}}^2\right)^3}. \tag{22}$$

This kernel as a function of $\phi_{\rm AB}$ is shown in Fig. 6. Clearly, the kernel has a sharp dip at $\phi_{\rm AB} = 0$ but changes its sign at $F_{\phi_{\rm AB}} = \pm 1/2$, namely, $\phi_{\rm AB} = \pm\frac{1}{2|s_{12}|}$. The width of the dips becomes very narrow as $|s_{12}|^{-1}$.

Using the obtained kernel, we can evaluate the pumped charge for the areas, $[a_{\rm min}, a_{\rm max}] = [-\infty, \infty]$ and $[-\phi_{\rm ABmax}, \phi_{\rm ABmax}]$,

$$q\left(\phi_{\rm ABmax}\right) \quad = \quad \frac{|s_{12}|}{2}\int_{-\phi_{\rm ABmax}}^{\phi_{\rm ABmax}} d\phi_{\rm AB}\left[\frac{(\frac{1}{4} - (2|s_{12}|\sin\frac{\phi_{\rm AB}}{2})^2)\cos\phi_{\rm AB}}{(\frac{1}{4} + (2|s_{12}|\sin\frac{\phi_{\rm AB}}{2})^2)^2} - \frac{\sin^2\frac{\phi_{\rm AB}}{2}}{\frac{1}{4} + (2|s_{12}|\sin\frac{\phi_{\rm AB}}{2})^2}\right]. \tag{23}$$

We then obtain analytical expressions for two extreme settings:

- $\phi_{\rm ABmax} = 1/(2\,|s_{12}|)$, where we take only the negative part of the dip, then

$$q\left(\frac{1}{2\,|s_{12}|}\right) \quad = \quad \frac{|s_{12}|}{2}\int_{-\frac{1}{2|s_{12}|}}^{\frac{1}{2|s_{12}|}} d\phi_{\rm AB}\left[\frac{(\frac{1}{4} - (2|s_{12}|\sin\frac{\phi_{\rm AB}}{2})^2)\cos\phi_{\rm AB}}{(\frac{1}{4} + (2|s_{12}|\sin\frac{\phi_{\rm AB}}{2})^2)^2} - \frac{\sin^2\frac{\phi_{\rm AB}}{2}}{\frac{1}{4} + (2|s_{12}|\sin\frac{\phi_{\rm AB}}{2})^2}\right]$$
$$\to 1 - \frac{3(\pi - 3)}{32\,|s_{12}|^2} + O\left(\frac{1}{|s_{12}|^4}\right), \tag{24}$$

  for $|s_{12}| \to \infty$. Therefore, the pumped charge per cycle is unity, which seems to correspond to the preceding result studied in a one-QD system with two potentials chosen as control parameters.[19]

- $\phi_{\rm ABmax} = \pi$, where we take both the negative and positive contributions around the dip,

$$q(\pi) \quad = \quad \frac{\pi}{2|s_{12}|}\left[\frac{(16|s_{12}|^2 + 1)^{3/2} - 24|s_{12}|^2 - 1}{(16|s_{12}|^2 + 1)^{3/2}} - \frac{1}{2}\left\{1 - \frac{1}{\sqrt{16|s_{12}|^2 + 1}}\right\}\right]$$
$$\to \frac{\pi}{4\,|s_{12}|}\ (\text{for } |s_{12}| \to \infty). \tag{25}$$

  Therefore, we do not expect the pumped charge when choosing a large area in the phase space since the positive and negative kernels cancel each other.

When $[a_{\rm min}, a_{\rm max}] = [-b, b]$ for finite $b > 0$ and $[-\phi_{\rm ABmax}, \phi_{\rm ABmax}]$, we could not obtain analytical results. Figure 7 shows a numerical estimation of the pumped charge as a function of $\phi_{\rm ABmax}$ for various values of b of $1, 10, 100$ and $|s_{12}| = 10$. Except for a very small $\phi_{\rm ABmax}$, the pumped charge is nearly constant, which enables the clear steplike behavior described in the previous section. However, the step height is not universal and depends on the range of the integration $[-b, b]$.

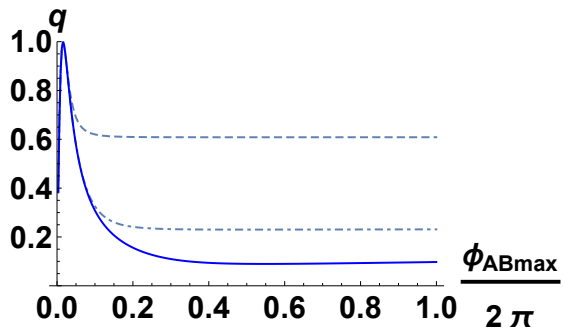

Fig. 7. (Color online) Pumped charge as a function of the varying range $[-\phi_{\mathrm{ABmax}}, \phi_{\mathrm{ABmax}}]$ and $[-b, b]$ for $b = 1$ (dashed), 10 (dot-dashed), and 100 (solid) for $|s_{12}| = 10$ (top) and $\beta = 1$.

5. Conclusions

We obtained explicit expressions for the pumped charge for a ring of three noninteracting quantum dots (QDs) using Brouwer's formula. We chose the energy of one QD and the Aharonov–Bohm phase determined by the flux penetrating through the ring $(\varepsilon_3, \phi_{\mathrm{AB}})$ as control parameters. We found that the pumped charge per cycle shows quasisinusoidal or steplike behavior depending on the energies of QDs 1 and 2, the tunnel couplings, and the variable range of the parameters. The step height is not universal and depends on the trajectory of the parameters. Explicit analytical expressions are obtained for the situation that the three QDs are weakly coupled with the leads, where the steplike behavior is related to the Fano resonance. For realizing a current standard, our results have an advantage since we can obtain large charges per cycle by changing the phase indefinitely. Moreover, from the viewpoint of the stability of the current standard against the fluctuations of the flux in the experiments, the steplike behavior found in the three-QD ring may enable the precise control of the pumped charge.

Acknowledgments

We thank T. Aono, S. Kawabata and S. Nakamura for useful comments and discussions. M. T. also thanks the Tsukuba Nanotechnology Human Resource Development Program. Part of this work was supported by JSPS KAKENHI (26247051).

Appendix: Kernel and pumped charge of three-QD ring

We consider the kernel of three-QD ring $\Pi(X_1, X_2)$. By definition, the retarded Green's function has the property $\mathbf{G}^{\mathbf{r}}(\mathbf{G}^{\mathbf{r}})^{-\mathbf{1}} = \mathbf{1}$. By differentiating this identity with respect to X, we

obtain

$$\frac{\partial \mathbf{G}^r}{\partial X} = -\mathbf{G}^r \mathbf{f}_X \mathbf{G}^r, \tag{A·1}$$

where we define the matrix $\mathbf{f}_X \equiv \partial \left(\mathbf{G}^{\mathbf{r}}\right)^{-1} / \partial X$. The kernel requires the $(1,1)$ and $(1,2)$ components of Eq. (A·1).

When we choose $X = \varepsilon_3$,

$$\mathbf{f}_{\varepsilon_3} = \begin{pmatrix} 0 & 0 & 0 \\ 0 & 0 & 0 \\ 0 & 0 & -1 \end{pmatrix}, \tag{A·2}$$

then

$$\left(\frac{\partial \mathbf{G}^r}{\partial \varepsilon_3}\right)_{11} = G^r_{13} G^r_{31}, \ \left(\frac{\partial \mathbf{G}^r}{\partial \varepsilon_3}\right)_{12} = G^r_{13} G^r_{32}. \tag{A·3}$$

When we choose $X = \phi_{12}$,

$$\mathbf{f}_{\phi_{12}} = \begin{pmatrix} 0 & -it_{12} & 0 \\ it_{21} & 0 & 0 \\ 0 & 0 & 0 \end{pmatrix}, \tag{A·4}$$

then

$$\left(\frac{\partial \mathbf{G}^r}{\partial \phi_{12}}\right)_{11} = iG^r_{11}\left(t_{12}G^r_{21} - t_{21}G^r_{12}\right), \left(\frac{\partial \mathbf{G}^r}{\partial \phi_{12}}\right)_{12} = i\left(t_{12}G^r_{11}G^r_{22} - t_{21}\left(G^r_{12}\right)^2\right). \tag{A·5}$$

Although we have chosen the tunneling phase ϕ_{12} as one of the control parameters, we found that the kernel depends only on the total sum of the tunneling phases: $\phi = \phi_{12}+\phi_{23}+\phi_{31}$. This result is invariant even if we choose other tunneling phases ϕ_{23} or ϕ_{31} as the control parameter. This is related to the electron coherence in the three-QD ring and gauge invariance. If one of the tunneling amplitudes t_{23} or t_{31} is zero, the phase coherence is not maintained along the ring, and the kernel may explicitly depend on ϕ_{12}. We can divide the phase ϕ into two parts, the AB phase from the magnetic flux penetrating through the ring ϕ_{AB} ($\phi_{\mathrm{AB}} = 2\pi\frac{\Phi}{\Phi_0}$, $\Phi_0 = \frac{h}{e}$) and the phase independent of the flux ϕ^*; $\phi = \phi_{\mathrm{AB}} + \phi^*$. Assuming that the QDs are made of *s*-orbitals, tunnel coupling provides lower energy for a symmetric orbital without nodes, and the tunnel amplitude should take a negative value $t_{12} = -|t_{12}|$. This corresponds to $e^{i\phi^*} = (-1)^3 = -1$, i.e., $\phi^* = \pi$. The phase that we can change freely is ϕ_{AB} from the flux penetrating through the ring and we regard ϕ_{AB} as a control parameter; thus the final form of the kernel is

$$\tilde{\Pi}\left(x_3, \phi_{\mathrm{AB}}\right) = \frac{|s_{12}|}{\pi |\Delta_3|^4} \mathrm{Im}\Big[2\sin\phi_{\mathrm{AB}} |s_{23}s_{31}|$$

$$\times\left\{|s_{12}s_{23}|\,e^{-i\phi_{\rm AB}}-|s_{31}|\left(x_2-\frac{i}{2}\right)\right\}\left\{|s_{12}s_{23}|\,e^{i\phi_{\rm AB}}-|s_{31}|\left(x_2-\frac{i}{2}\right)\right\}\left\{\left(x_2+\frac{i}{2}\right)x_3-|s_{23}|^2\right\}$$
$$-ie^{i\phi_{\rm AB}}\left\{|s_{12}s_{23}|\,e^{-i\phi_{\rm AB}}-|s_{31}|\left(x_2-\frac{i}{2}\right)\right\}\left\{|s_{12}s_{31}|\,e^{-i\phi_{\rm AB}}-|s_{23}|\left(x_1-\frac{i}{2}\right)\right\}$$
$$\times\left(\left\{\left(x_2+\frac{i}{2}\right)x_3-|s_{23}|^2\right\}\left\{\left(x_1+\frac{i}{2}\right)x_3-|s_{31}|^2\right\}-\left(|s_{31}s_{23}|\,e^{-i\phi_{\rm AB}}-|s_{12}|\,x_3\right)^2\right)\Bigg], \qquad \text{(A·6)}$$

where Δ_3 is the determinant of the retarded Green's function given in Eq. (10) and given by

$$\Delta_3 = \left(x_1+\frac{i}{2}\right)\left(x_2+\frac{i}{2}\right)x_3+2\,|s_{12}s_{23}s_{31}|\cos\phi_{\rm AB}-|s_{23}|^2\left(x_1+\frac{i}{2}\right)-|s_{31}|^2\left(x_2+\frac{i}{2}\right)-|s_{12}|^2\,x_3. \qquad \text{(A·7)}$$

References

1) M. G. Vavilov, V. Ambegaokar, and I. L. Aleiner, Phys. Rev. B **63**, 195313 (2001).
2) B. Hiltscher, M. Governale, and J. König, Phys. Rev. B **81**, 085302 (2010).
3) D. V. Averin, M. Möttönen, and J. P. Pekola, Phys. Rev. B **84**, 245448 (2011).
4) J. D. Sau, T. Kitagawa, and B. I. Halperin, Phys. Rev. B **85**, 155425 (2012).
5) T. Yuge, T. Sagawa, A. Sugita, and H. Hayakawa, Phys. Rev. B **86**, 235308 (2012).
6) S. Nakajima, M. Taguchi, T. Kubo, and Y. Tokura, Phys. Rev. B **92**, 195420 (2015).
7) G. P. Lansbergen, Y. Ono, and A. Fujiwara, Nano Lett. **12**, 763 (2012).
8) J. P. Pekola, O. P. Saira, V. F. Maisi, A. Kemppinen, M. Möttönen, Y. A. Pashkin, and D. V. Averin, Rev. Mod. Phys. **85**, 1421 (2013).
9) Y. Nagamune, H. Sakaki, L. P. Kouwenhoven, L. C. Mur, C. J. P. M. Harmans, J. Motohisa and H. Noge, Appl. Phys. Lett. **64**, 2379 (1994).
10) D. J. Thouless, Phys. Rev. B **27**, 6083 (1983).
11) M. Büttiker, H. Thomas, and A. Prêtre, Z. Phys. B **94**, 133 (1994).
12) P. W. Brouwer, Phys. Rev. B **58**, R10135 (1998).
13) M. Switkes, C. M. Marcus, K. Campman, and A. C. Gossard, Science **283**, 1905 (1999).
14) P. W. Brouwer, Phys. Rev. B **63**, 121303(R) (2001).
15) M. L. Polianski and P. W. Brouwer, Phys. Rev. B **64**, 075304 (2001).
16) L. DiCarlo, C. M. Marcus, and J. S. Harris, Jr., Phys. Rev. Lett. **91**, 246804 (2003).
17) C. Benjamin, Eur. Phys. J. B **52**, 403 (2006).
18) C. Benjamin, Appl. Phys. Lett. **103**, 043120 (2013).
19) Y. Levinson, O. Entin-Wohlman, and P. Wölfe, Physica A **302**, 335 (2001).
20) Y. Wei, J. Wang, and H. Guo, Phys. Rev. B **62**, 9947 (2000).
21) O. Entin-Wohlman and A. Aharony, Phys. Rev B **66**, 035329 (2002).
22) M. Moskalets and M. Büttiker, Phys. Rev. B **64**, 201305(R) (2001).
23) J. N. H. J. Cremers and P. W. Brouwer, Phys. Rev. B **65**, 115333 (2002).
24) J. E. Avron, A. Elgart, G. M. Graf, and L. Sadun, Phys. Rev. B **62**, R10618 (2000).
25) R. Bustos-Marún, G. Refael, and F. von Oppen, Phys. Rev. Lett. **111**, 060802 (2013).
26) B. D. Josephson, Phys. Lett. **1**, 251 (1962).

27) Appendix D, J. Splettstoesser, Dr. Thesis, Faculty of Physics and Astronomy, Ruhr-Universität Bochum, 2007 (available at http://www-brs.ub.ruhr-uni-bochum.de/netahtml/HSS/Diss/SplettstoesserJanine/).

28) A. N. Ageev, S. Yu. Davydov, and A. G. Chirkov, Tech. Phys. Lett. **36**, 392 (2000). Translated from Pis'ma v Zhurnal Teknicheskol Fiziki **26**, 70 (2000).

29) K. Moulopoulos, J. Phys. A: Math. Theor. **43**, 354019 (2010).

30) T. Kalvola and P. Stovicek, Ann. Phys. **326**, 2702 (2011).

31) S. Russo, J. Tobiska, T. M. Klapwijk, and A. F. Morpurgo, Phys. Rev. Lett. **99**, 086601 (2007).

32) B. Lee, E. Yin, T. K. Gustafson, and R. Chiao, Phys. Rev. A **45**, 4319 (1992).

33) L. Arrachea, Phys. Rev. B **66**, 045315 (2002).

34) L. Arrachea, Phys. Rev. B **70**, 155407 (2004).

35) L. E. F. Foa Torres, Phys. Rev. B **72**, 245339 (2005).

36) D. S. Fisher and P. A. Lee, Phys. Rev. B **23**, 6851 (1981).

37) T. K. Ng and P. A. Lee, Phys. Rev. Lett. **61**, 1768 (1988).

38) L. Arrachea and M. Moskalets, Phys. Rev. B **74**, 245322 (2006).